

## INDUCED CURRENTS ON INFINITE PEC CYLINDERS EXCITED BY GAUSSIAN PULSE: AN APPLICATION OF CFD-BASED ALGORITHMS

MingTsu Mark Ho<sup>1</sup>, John H. Beggs<sup>2</sup>, J. Patrick Donohoe<sup>3</sup>

<sup>1</sup>Dept. of Electronic Eng., Wu-Feng Institute of Tech. & Commerce, Taiwan; homt@sun5.wfc.edu.tw

<sup>2</sup>Electronics Engineer, Microwave Systems Branch, NASA/GSFC; beggs@jazzman.gsfc.nasa.gov

<sup>3</sup>Dept. of Electrical & Computer Eng., Mississippi State University; donohoe@ece.msstate.edu

### I. INTRODUCTION

The computational electromagnetics technique providing numerical solutions to Maxwell's equations plays a very important role in helping to understand the general characteristics and physics of various electromagnetic field problems. Two widely used methods to solve Maxwell's equations are the method of moments and the Yee algorithm.

The moment method, the first computational electromagnetics technique, was developed for solving electromagnetic problems. The method of moment numerically determines currents on the object's surface in the frequency domain by solving the appropriate integral equation in a systematic fashion [1-3]. In 1966, Yee successfully applied a second-order accurate central-difference method for direct numerical solutions of the time-dependent Maxwell's equations [4]. The finite difference-time domain technique provides time-domain solutions by using central difference scheme in both time and space. Beggs uses surface impedance boundary conditions on the object surface, allowing larger cells to be used and then reduces the storage requirement when modeling lossy dielectric objects [5].

The computational fluid dynamics (CFD) method is a powerful approach for solving the Euler and Navier-Stokes equations. It produces accurate numerical data obtained in a general boundary conforming curvilinear coordinate system. For the reasons given below, the application of CFD-based algorithms to the solutions of Maxwell's equations involving objects with complex curves seems to have a promising future. First, Maxwell's equations can be cast into the same form as the Euler equations. Secondly, accurate solutions of the Euler equations governing fluid dynamic problems are obtained through successful applications of CFD algorithms.

### II. GOVERNING EQUATIONS AND TRANSVERSE MAGNETIC GAUSSIAN PULSE

The time-domain governing equations in source-free regions are the Maxwell's equations:

$\frac{\partial \mathbf{B}}{\partial t} + \nabla \times \mathbf{E} = 0$ ,  $\frac{\partial \mathbf{D}}{\partial t} - \nabla \times \mathbf{H} = 0$ . Given the two-dimensional formulation (no z-variation), the transformation of the time-invariant curvilinear coordinate system, Maxwell's equations become  $\frac{\partial \mathbf{Q}}{\partial \tau} + \frac{\partial \mathbf{F}}{\partial \xi} + \frac{\partial \mathbf{G}}{\partial \eta} = 0$  where  $\tau = t$ ,  $\mathbf{Q} = \mathbf{J}_q$ ,  $\mathbf{F} = \mathbf{J}(\xi_x \mathbf{f} + \xi_y \mathbf{g})$ ,  $\mathbf{G} = \mathbf{J}(\eta_x \mathbf{f} + \eta_y \mathbf{g})$ , and  $\mathbf{J}$  is the Jacobian of the

inverse transformation and three vectors are defined as

$$\mathbf{q} = [B_x, B_y, D_z]^T, \quad \mathbf{f} = \left[ 0, -\frac{D_z}{\epsilon}, -\frac{B_y}{\mu} \right]^T, \quad \mathbf{g} = \left[ \frac{D_z}{\epsilon}, 0, \frac{B_x}{\mu} \right]^T.$$

In this study, the incident field is assumed to be TM plane electromagnetic fields in the form of Gaussian pulse traveling along the x-axis. This time-domain pulse is truncated by a rectangular window with a cut-off level of 80 dB below the peak value and its width  $T$  is defined as one half of the width where the magnitude is about 60.6% ( $e^{-1/2}$ ) of the peak value.

### III. NUMERICAL METHOD AND BOUNDARY CONDITIONS

After applying the central difference operator, the flux vector splitting technique, and the Newton sub-iterative method to the above equation, an implicit numerical procedure of second order accuracy in time and third order accuracy in space is given as

$$\left[ I + \frac{2}{3} \Delta\tau (\mathbf{M}^+ \bullet + \mathbf{M}^- \bullet)^{m-1} \right] \Delta\mathbf{Q}^m = \left[ \mathbf{Q}^{m-1} - \mathbf{Q}^n + \frac{2}{3} \Delta\tau \mathbf{R}^{m-1} + \frac{1}{3} \Delta\mathbf{Q}^{n-1} \right].$$

As shown, the superscript  $\mathbf{n}$  indicates the time level while  $\mathbf{m}$  is the number of Newton sub-iteration, the vector  $\{\mathbf{Q}^m\}$  is used for  $\{\mathbf{Q}^{n+1}\}$  as the  $m^{\text{th}}$  sub-iterative result which is generated from the initial guess vector  $\{\mathbf{Q}^{m=0}\} = \{\mathbf{Q}^n\}$ . The residual term is written as  $\mathbf{R} = \delta_i \mathbf{F} + \delta_j \mathbf{G}$  with the central difference operator being  $\delta_k (*) = (* )_{k+1/2} - (* )_{k-1/2}$ . Furthermore,  $\mathbf{M}^\pm \bullet = (\delta_i \mathbf{A}^\pm \bullet + \delta_j \mathbf{B}^\pm \bullet)$  and the central difference operator operates on the products of  $(\mathbf{A}^\pm \Delta\mathbf{Q})$  and  $(\mathbf{B}^\pm \Delta\mathbf{Q})$ .

The application of appropriate boundary conditions determines the accuracy of any numerical solver. In the present algorithm, the boundary conditions are derived from the concept of characteristic variables and are known as the characteristic variable boundary conditions. By definition, every characteristic variable defines the direction and speed of the information propagation. For instance, the characteristic variable associated with the zero eigenvalue can be interpreted as the normal component of the total flux densities that must vanish on a PEC surface or continue across the interface between any two dielectric materials.

### IV. RESULTS

The induced currents on an infinite PEC cylinder shown in this section are obtained from the present algorithm, the Yee algorithm, and the analytic expression, respectively. Prior to the study of currents on a circular cylinder, a cylinder with square cross-section is modeled. Reasons for so doing are: to investigate the feasibility of approximating a circular cylinder by a multi-sided cylinder having compatible dimensions and to examine the effects of grid structure on the results.

There are five various currents sampled around a circular cylinder for comparisons. The five sampling locations are  $0^\circ$ ,  $45^\circ$ ,  $90^\circ$ ,  $135^\circ$ , and  $180^\circ$ , respectively. For the case where the incident pulse is initially set to propagate in the positive-x direction toward the cylinder, the  $0^\circ$ -position would be on

the shadow side while the 180°-position is facing the incident. For the square cylinder this five locations are reduced to three, namely, 0°, 90°, and 180°. In order to preserve the scheme accuracy, it is necessary to modify the O-type grid by doubling the number of points from one block to the next as the grid is built radially outward.

Figures 1 and 2 show the induced currents on a 12 cm by 12 cm square cylinder under the illumination of a Gaussian pulse with  $T = 0.45$  ns. The analytic solutions are obtained based on a circular cylinder whose diameter is 12 cm. Reasonable agreements among the CFD-based, the Yee algorithms, and the exact values are observed for this model.

Further comparisons for different dimensions of both the cylinder and the pulse are given below. Under the same conditions, a circular cylinder with 25 cm in radius is modeled by the CFD-based approach and plotted in Figure 3. As a final case, another circular cylinder with radius of 20 cm is excited by a Gaussian pulse of  $T = 0.2$  ns whose results are given in Figure 4. Better agreement in the latter plot indicates that the resolution is affected by the relative size of the target and the width of the excitation.

## V. CONCLUSION

The CFD-based algorithm produces results that are in good agreement with both the analytic values and the Yee algorithm. It is also found from this study that in order to obtain more accurate solutions from the CFD-based approach, the greater dimension of target or the narrower pulse duration is preferable. The grid structure was found not to significantly affect the numerical results from the present study. As implied earlier, the present numerical algorithm is also expected to have the capability of solving electromagnetic field scattering problems involving complex geometries that have to be modeled using a three-dimensional formulation.

## REFERENCES

- [1] J. Patrick Donohoe, C. D. Taylor, MingTsu Ho, A report submitted to U.S. Army Missile Command, AMSMI-RD-WS-UB, December 1992.
- [2] J. Patrick Donohoe, C. D. Taylor, MingTsu Ho, "Induced currents on slotted bodies of revolution under plane wave illumination," IEEE SOUTHEASTCON 1996.
- [3] J. Patrick Donohoe, C. D. Taylor, MingTsu Ho, "Response of an open-ended slotted body of revolution to an ultra-wideband electromagnetic pulse," 1997 IEEE AP-S International Symposium and URSI Radio Science Meeting.
- [4] K. S. Yee, "Numerical solution of initial boundary value problems involving Maxwell's equations in isotropic media," IEEE Trans. Antennas Propagation, vol. AP-14, pp.302-307, May 1966.
- [5] J. H. Beggs, "Finite-difference time-domain implementation of surface impedance boundary conditions in one, two, and three dimensions," Ph.D. Dissertation, Pennsylvania State University, May 1993.

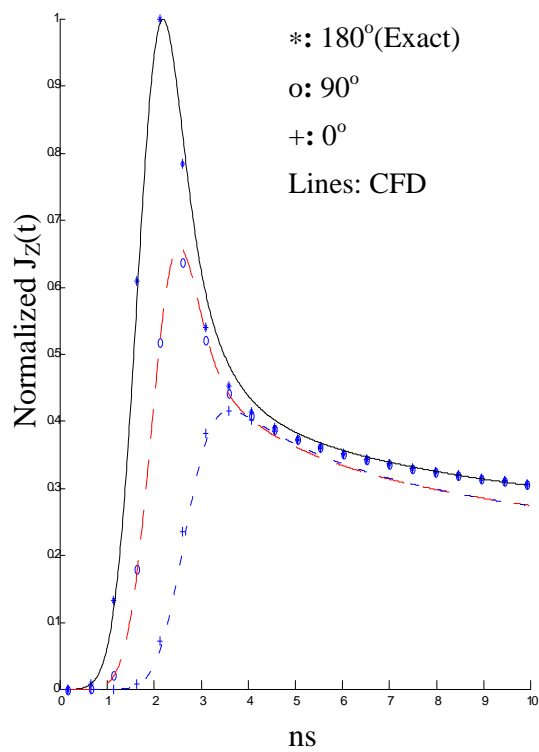


Figure 1. Induced currents on cylinders: CFD ( $12 \text{ by } 12 \text{ cm}^2$ ) vs. Exact ( $r=6\text{cm}$ ).

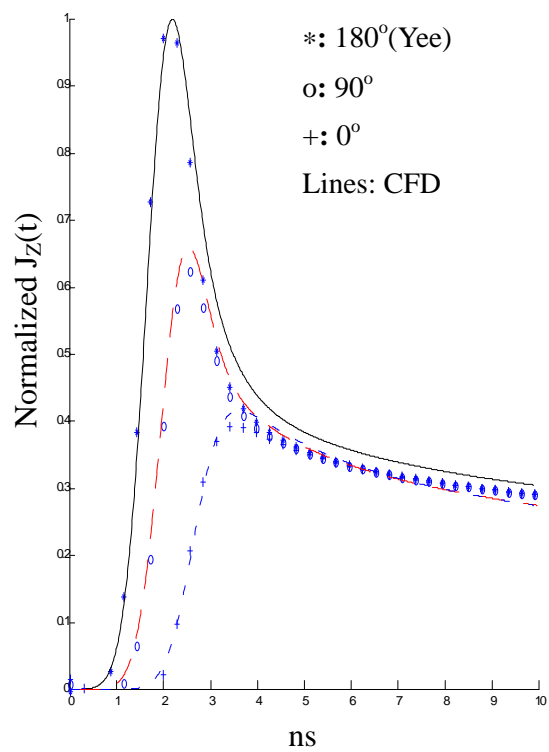


Figure 2. Induced currents on a ( $12 \text{ by } 12$ )  $\text{cm}^2$  cylinder: CFD vs. Yee.

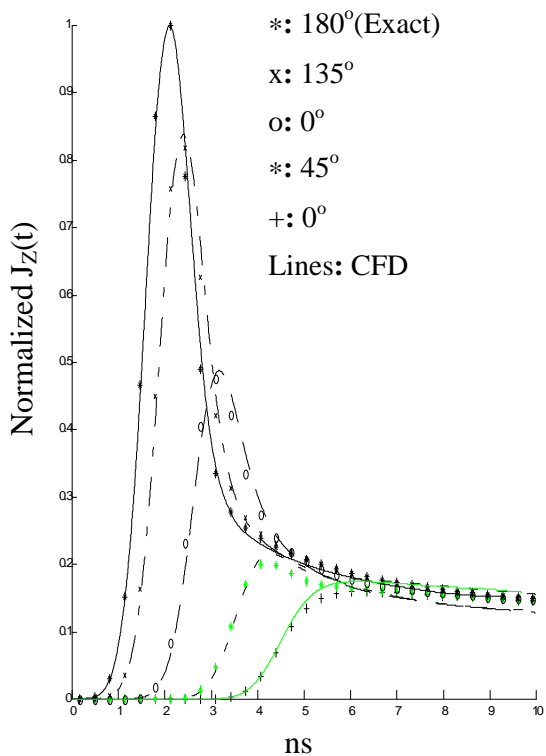


Figure 3. Induced currents on a circular cylinder ( $r=25\text{cm}$ ,  $T=0.45\text{ns}$ ): CFD vs. Exact.

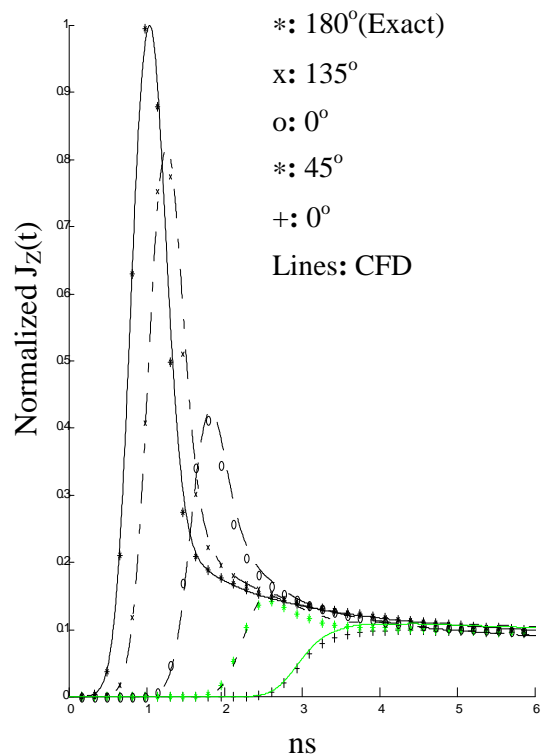


Figure 4. Induced currents on a circular cylinder ( $r=20\text{cm}$ ,  $T=0.20\text{ns}$ ): CFD vs. Exact.